Experimental Study of Stationary Shoulder Friction Stir Welded 7N01-T4 Aluminum Alloy

S.D. Ji, X.C. Meng, Z.W. Li, L. Ma, and S.S. Gao

Stationary shoulder friction stir welding (SSFSW) was successfully used to weld 7N01-T4 aluminum alloy with the thickness of 4 mm. Effects of welding speed on formations, microstructures, and mechanical properties of SSFSW joint were investigated in detail. Under a constant rotational velocity of 2000 rpm, defect-free joints with smooth surface and small flashes are attained using welding speeds of 20 and 30 mm/min. Macrostructure of nugget zone in cross section presents kettle shape. For 7N01-T4 aluminum alloy with low thermal conductivity, decreasing welding speed is beneficial to surface formation of joint. With the increase of welding speed, mechanical properties of joints firstly increase and then decrease. When the welding speed is 30 mm/min, the tensile strength and elongation of joint reach the maximum values of 379 MPa and 7.9%, equivalent to 84.2 and 52% of base material, respectively. Fracture surface morphology exhibits typical ductile fracture. In addition, the minimum hardness value of joint appears in the heat affected zone.

1. Introduction

7N01 aluminum alloy, as one of high strength aluminum alloys, has been widely applied to high speed train because of the advantages of high strength, excellent corrosion resistance, and good weldability. However, when fusion welding is used to weld 7N01 aluminum alloy, hot crack, porosity, and lack of fusion easily appear in the joint, which degrades the mechanical properties and restricts the wide application (Ref 1-4). As a solid-state joining technique, friction stir welding (FSW) owns the benefits of high joint strength, low distortion, no fusion welding defects, low power consumption, and non-pollution (Ref 1, 5). Therefore, FSW has potential to weld 7000 series alloys (Ref 3-7). Meng et al. (Ref 6) performed FSW of 7N01 alloy successfully and obtained the maximum tensile strength of 340 MPa. Han et al. (Ref 7) found that the pin with screw was beneficial to increase mechanical property of 15 mm thick 7N01 alloy joint. However, arc corrugation and large shoulder affected zone (SAZ) appear in the traditional FSW joint, which is detrimental to the mechanical property (Ref 3, 6, 7).

Stationary shoulder friction stir welding (SSFSW) is a novel joining technique derived from traditional FSW, which is mainly composed of outer stationary shoulder and inner rotational tool (Ref 8-11). During SSFSW process, the stationary shoulder frictionally slides over joint top surface and forges joint, while the inner rotational tool rotates and then generates frictional heat, making the material in nugget zone (NZ) sufficiently softened and stirred. Choosing 2219-T6 aluminum alloy as research object, Liu et al. (Ref 8, 9) obtained SSFSW joint with smooth surface and small thickness reduction. Li et al. (Ref 10) and Ji et al. (Ref 11) respectively carried out SSFSW of 6061 and 6005A aluminum alloys and found that SSFSW joint owned narrower heat affected zone (HAZ) and SAZ compared with traditional FSW. Li et al. (Ref 4) also obtained high quality SSFSW joint of 7075 aluminum alloy. However, up to present, SSFSW of 7N01 alloy is still not reported. In this study, SSFSW experiment of 7N01-T4 aluminum alloy was carried out in order to attain FSW joint with smooth surface and high quality, which is beneficial to the engineering application of 7N01 alloy and the development of SSFSW process.

2. Experimental Procedures

The base material (BM) used in this study was 7N01-T4 aluminum alloy plate, whose dimensions were $500 \times 100 \times 4$ mm^3. The experiment of SSFSW was performed using a FSW machine (FSW-3LM-4012) with self-designed SSFSW tool system which consisted of stationary shoulder and inner rotational tool, as shown in Fig. 1. The outer and inner diameters of stationary shoulder are 14 and 6.3 mm, respectively. The inner rotational tool is composed of small plane shoulder and right-screwed pin. The diameters of shoulder, pin bottom, and pin tip are respectively 6, 5, and 3 mm. The length of pin is 3.8 mm. Meanwhile, the plunge depth of stationary shoulder was 0.2 mm and the tilt angle with respect to Z-axis was 2.5°. In order to ensure sufficient heat input, the combination of high rotational velocity of 2000 rpm and low welding speeds varying from 20 to 70 mm/min are adopted during FSW process. Before welding, the plates to be welded were burnished by abrasive paper and cleaned using acetone in order to wipe off oxide layer.

After welding, the specimens were cut perpendicular to the welding direction using an electrical discharge cutting machine

S.D.Ji, X.C.Meng, Z.W.Li, L.Ma, and S.S.Gao, Faculty of Aerospace Engineering, Shenyang Aerospace University, No. 37 Daoyi South Avenue, Daoyi Development District, Shenyang 110136, China. Contact e-mail: superjsd@163.com.

to carry out the mechanical test and microstructural characterization. The microstructural feature was observed by an optical microscope (OLYMPUS, GX71) after etched by Keller's reagent. Meanwhile, average grain size of joint was estimated according to GB/T 6394-2002 (ASTM E112-1996) (Ref 12). To evaluate mechanical property of SSFSW joint, three tensile specimens were prepared for each joint with reference to GB/T 2651-2008 (equivalent to ISO 9016: 2001) (Ref 13). The average value was presented for discussion. In addition, tensile test at room temperature was performed at a constant crosshead speed of 5 mm/min. Microhardness value of joint was measured by a microhardness tester at a load of 200 g for 10 s and the interval between two measured points was 0.5 mm. Fracture surface of tensile specimen was observed by scanning electron microscopy (SEM, KYKY-2800B). In order to recognize constituent particles, elemental analysis was performed using an energy dispersive x-ray spectroscopy (EDX) of SEM.

3. Results and Discussion

3.1 Surface Formation of Joint

Figure 2 indicates macroscopic appearance of SSFSW butt joint using the welding speed of 30 mm/min and rotational velocity of 2000 rpm. It is observed that the joint with smooth surface and smaller flashes is obtained, where a keyhole remaining at the end of joint resulted from the retraction of rotational tool. During SSFSW process, with the rotation and advancement of inner rotational tool, the arc corrugation and flashes form behind rotational tool (Ref 1, 10). However, the outer stationary does not rotate and slides over the surface of joint, eliminating arc corrugation. Moreover, stationary shoulder can effectively prevent plasticized material from flowing
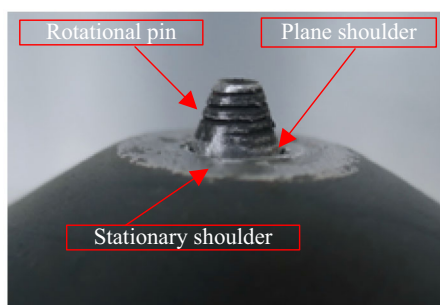

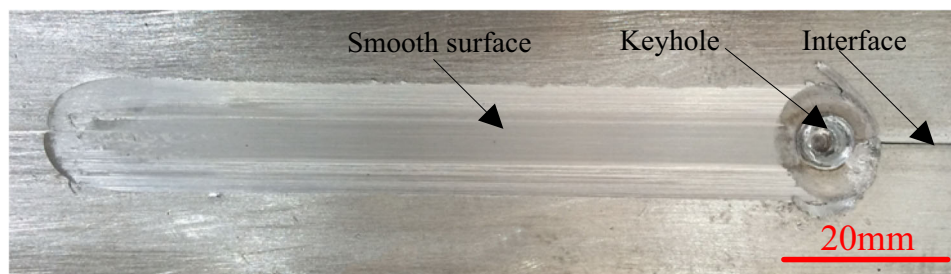Fig. 1 SSFSW tool used in the experiment

out of joint, decreasing flash size. The above-mentioned advantages are not only beneficial to both fatigue property and corrosion resistance, but also reduce postweld treatment for arc corrugation and flashes (Ref 9, 10).

Partial magnified photos of surface formation of SSFSW joints under different welding parameters are shown in Fig. 3. When welding speeds are respectively 20 and 30 mm/min, the smooth surface formation can be obtained, as exhibited in Fig. 3(a) and (b). Surface formation of SSFSW joint can be divided into rotational tool affected zone (RTAZ) and stationary shoulder affected zone (SSAZ), as shown in Fig. 3(d). During SSFSW process, the materials in the RTAZ experience higher frictional heat generated by friction between rotational tool and workpieces, which easily makes materials reach sufficient plasticized state. Therefore, as the stationary shoulder slides over the surface of RTAZ, the arc corrugation induced by inner rotational tool is easily eliminated and then smooth surface is attained. However, materials in the SSAZ only experience little heat attributed to heat transfer from the RTAZ. In fact, stationary shoulder is thought to heat sink, resulting in low temperature (Ref 4). Therefore, it is difficult to soften the materials located in the SSAZ. The friction between stationary shoulder and workpieces is similar to dry friction, which may lead to the formation of rough surface. From Fig. 3, it is seen that the surface formation of SSAZ at 40 mm/min (Fig. 3c) becomes coarse compared with that at 30 mm/min, while the surface formations at 50 and 70 mm/min are coarser (Fig. 3d and e).

In our pre-experiment, the phenomenon of rough surface did not appear in the SSFSW joint of 6061 aluminum alloy under the welding speed of 50 mm/min and rotational velocity of 2000 rpm (Ref 11). As a matter of fact, thermal conductivity of 7N01 aluminum alloy is lower than that of 6061 aluminum alloy. The thermal conductivities of 7N01 aluminum alloy and 6061 aluminum alloy at the temperature 500 °C which is easy to reach during FSW process are 170 and 195 W/(m K), respectively (Ref 14, 15). In addition, the hardness of 7N01 aluminum alloy is also higher than that of 6061 aluminum alloy. This is the good evidence that the hardness values of 7N01 alloy and 6061 alloy at room temperature are 135 and 98 Hv, respectively (Ref 6, 9). So, rough surface of SSAZ is not occurred in 6061 alloy welding joint (Ref 11). During SSFSW process, when higher welding speed or lower rotational velocity is employed, not only lower heat input but also shorter heat transfer time goes against softening the materials in SSAZ, leading to the coarse surface, as indicated in Fig. 3(c)-(f). In other words, for 7N01 aluminum alloy, the combination of low welding speed and high rotational velocity is essential in order to get the smooth surface of SSFSW joint (Table 1).
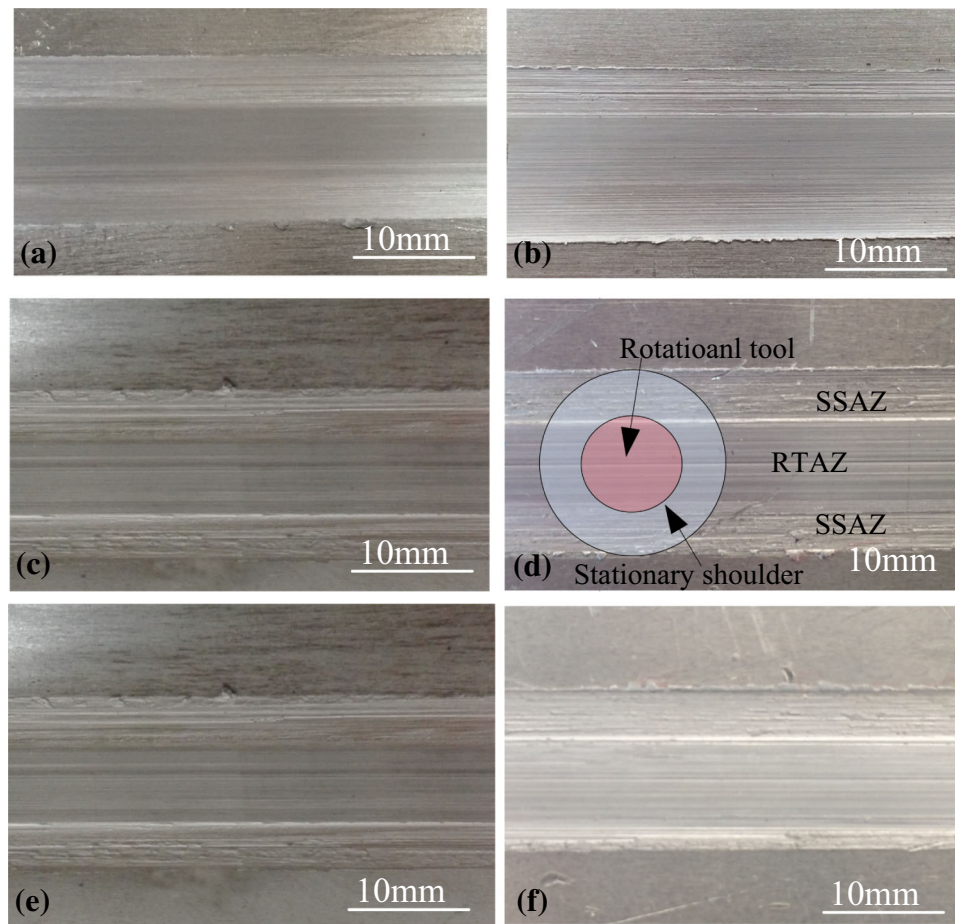

Fig. 2 Macroscopic appearance of SSFSW butt joint under the welding speed of 30 mm/min and rotational velocity of 2000 rpm

Fig. 3 Partial magnified photos of surface formation of SSFSW joints under different welding parameters at the rotational velocity of 2000 rpm: (a) 20 mm/min, (b) 30 mm/min, (c) 40 mm/min, (d) 50 mm/min, and (e) 70 mm/min; at the rotational velocity of 1800 rpm: (f) 30 mm/min

Table 1   Nominal chemical compositions of 7N01 aluminum alloy (mass fraction, %)

Alloy	Si	Fe	Cu	Mn	Mg	Cr	Zn	Ti	Al
7N01	0.3	0.35	0.2	$0.2 \sim 0.7$	1.0-2.0	0.3	4.0-5.0	0.2	Balance

3.2 Macrostructure and Microstructure of Joint

Macrostructures of SSFSW joints using different welding speeds at a constant rotational velocity of 2000 rpm are indicated in Fig. 4. It is seen that defect-free joints can be obtained at the welding speeds of 20 and 30 mm/min (Fig. 4a and b). NZ in cross section presents typical kettle shape which is different from the bowl shape reported by Li et al. (Ref 9). During SSFSW process, the morphology of joint mainly depends on welding parameters and shape of rotational tool (Ref 1). For fixed welding parameters, rotational tool plays a significant role in morphology. In this paper, as the right-screwed pin rotates anti-clockwise, materials in NZ flow towards and accumulate at the bottom of NZ (Ref 16). Consequently, due to combined effects of the supporting of backing plate and forging of stationary shoulder, materials at the bottom of NZ flow upwards again, which makes the materials assemble in the middle of NZ, leading to the formation of kettle shape. The NZ at 20/min is bigger than

that at 30 mm/min. This is because that lower welding speed is propitious to increase heat input and soften the materials surrounded in the rotational tool, obtaining bigger NZ. When the welding speed further increases to 40, 50, or 70 mm/min, defect occurs at the interface between rotational shoulder affected zone (RSAZ) and thermo mechanically affected zone (TMAZ). The reason is that the further increase of welding speed easily causes inadequate heat input and then leads to insufficient material flow, forming cavity defect, as shown in Fig. 4(c), (d), and (e). The partial enlarged photos are indicated in Fig. 5. In addition, rotational direction of rotational tool plays a significant role in joint quality. For the right-screwed pin used in this experiment, the anti-clockwise is better than clockwise. When the right-screwed pin rotates clockwise, materials in NZ flow towards top surface of joint (Ref 16), which results in the loss of plasticized material due to the gap between stationary shoulder and rotational tool, leading to the formation of cavity defect, as exhibited in Fig. 4(f).
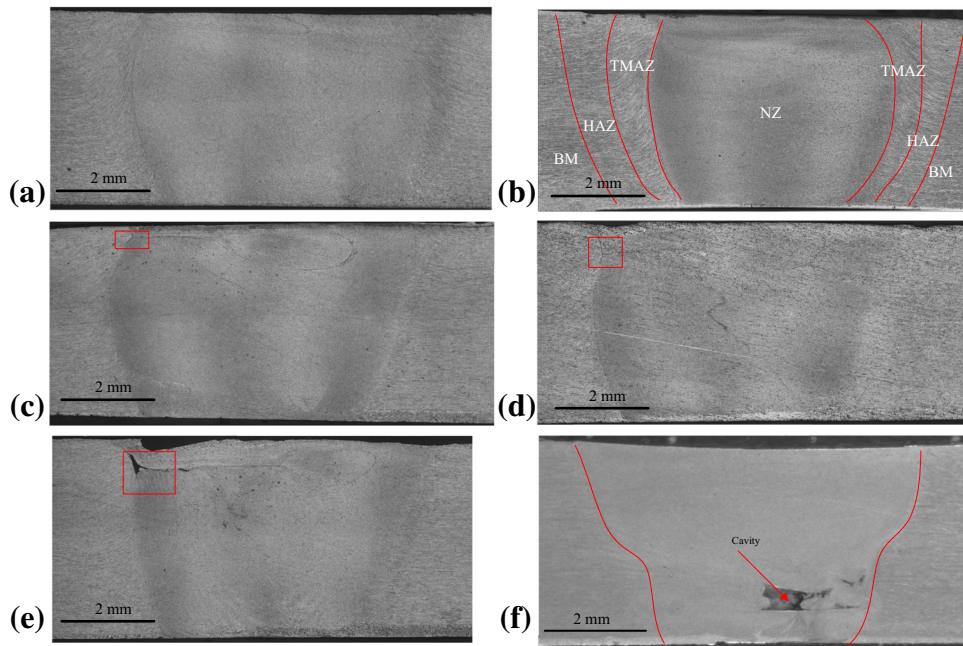
Fig. 4 Macrostructures of joint at rotational velocity of 2000 rpm: anti-clockwise: (a) 20 mm/min, (b) 30 mm/min, (c) 40 mm/min, (d) 50 mm/min, and (e) 70 mm/min; clockwise: (f) 30 mm/min
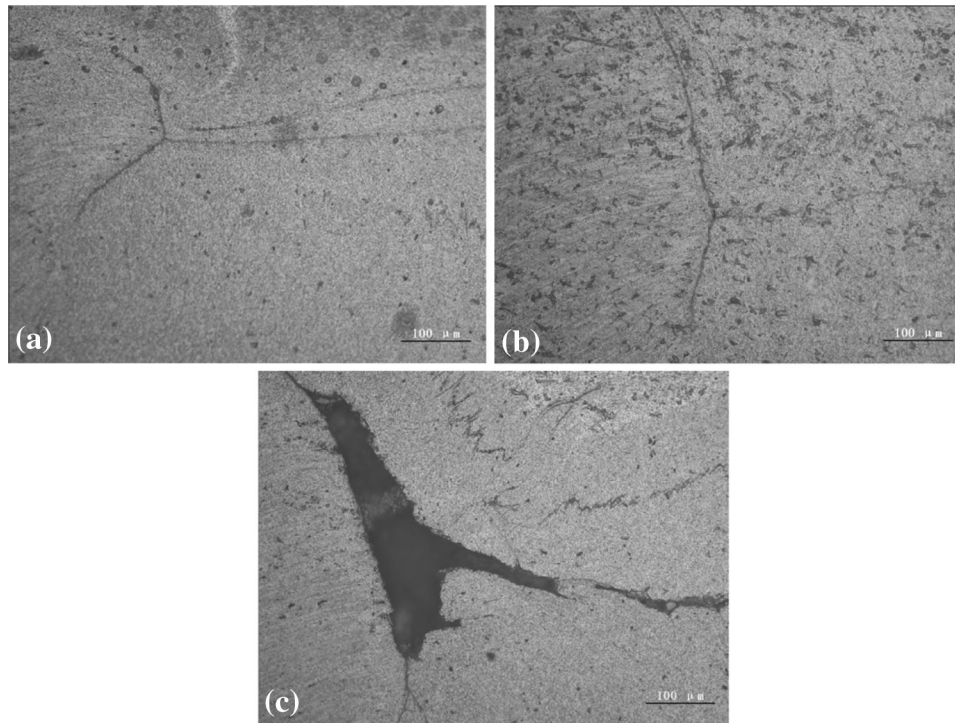

Fig. 5 Welding defect of joints under different welding speeds marked by square in Fig. 4: (a) 40 mm/min, (b) 50 mm/min, and (c) 70 mm/min

Similar to traditional FSW, the SSFSW joint is also divided into four zones: BM, TMAZ, HAZ, and NZ (Ref 1, 16), as indicated in Fig. 4(b). Microstructures of different positions of 7N01 alloy SSFSW joint at 30 mm/min are presented in Fig. 6. BM displays the elongated lath-shaped grains because of the rolling process (Fig. 6a). NZ is characterized by fine and equiaxed microstructures, which is due to dynamic recrystallization resulted from higher peak temperature and stain rate (Fig. 6b) (Ref 1, 17, 18). The grain size of NZ is about 16.3 μm. TMAZ is featured by deformed and elongated grains experienced thermal cycle and mechanical effects, as shown in Fig. 6(c)-(f). Different from traditional FSW, the obvious
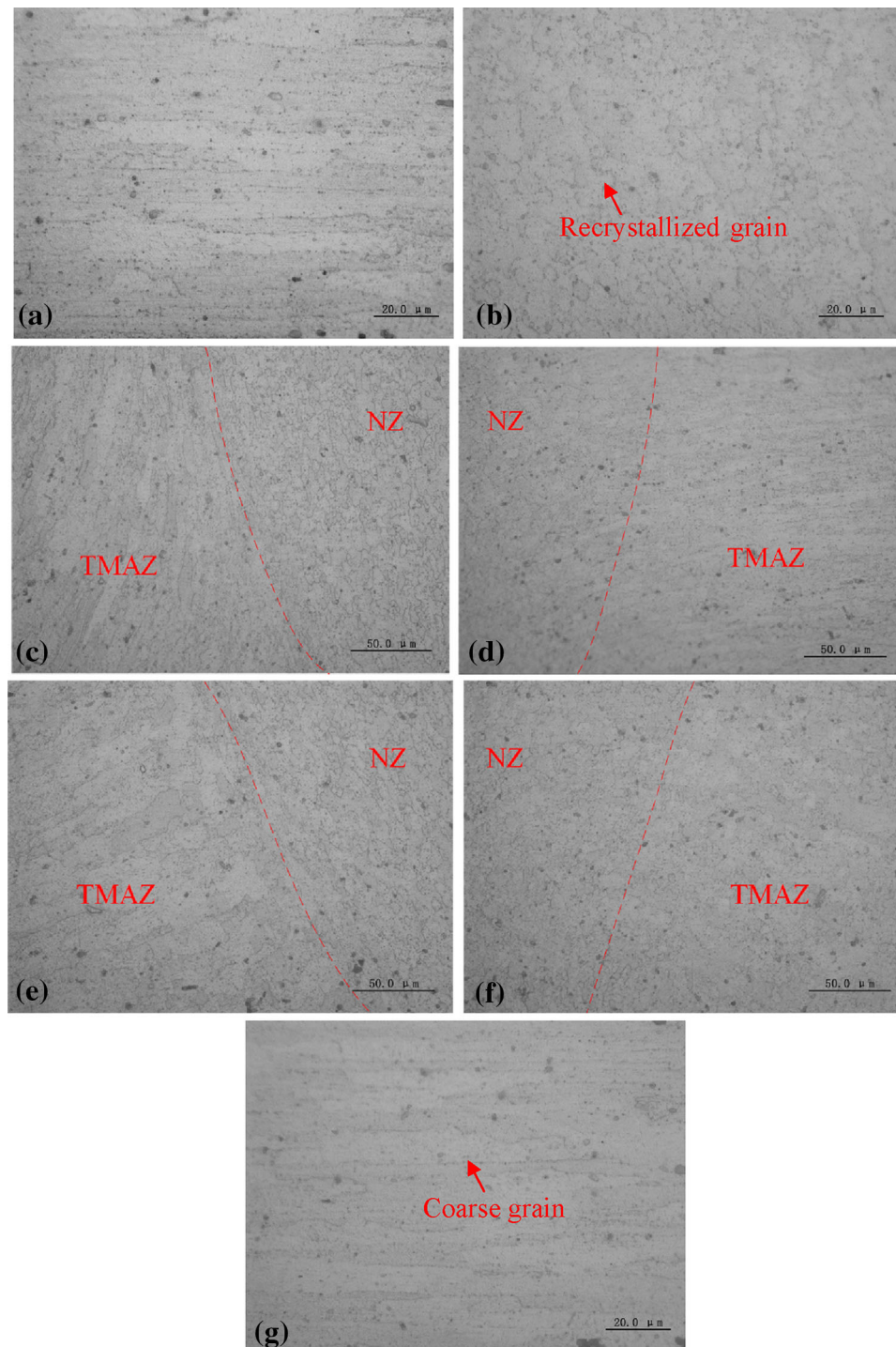
Fig. 6 Microstructures of different positions of joint at the welding speed of 30 mm/min: (a) BM, (b) NZ, (c) upper of TMAZ of AS, (d) upper of TMAZ of RS, (e) lower of TMAZ of AS, (f) lower of TMAZ of RS, and (g) HAZ

difference of TMAZ of 7N01 alloy SSFSW joint between advancing side (AS) and retreating side (RS) disappears. This phenomenon is also reported by Li et al. (Ref 4). In addition, the material at the top of joint suffers from more frictional heat than that at the bottom because of small rotational plane shoulder. Therefore, the materials at the top are prone to own better plastic flow behavior, which causes that the degree of plastic deformation at the top of TMAZ is bigger than that at the bottom. HAZ only experiences thermal cycle without

plastic deformation, which is filled with coarsened grains compared with BM (Fig. 6g). It is known that 7N01 aluminum alloy is an age-hardenable alloy which is strengthened by precipitation during heat treatment. In this study, in order to better understand precipitations, the EDX experiments were performed. The results are shown in Fig. 7. Therefore, it can be inferred that the precipitation in 7N01-T4 alloy is mainly AlCuFe containing phase. The result also accords with conclusion of Li et al. (Ref 4). In addition, compared with
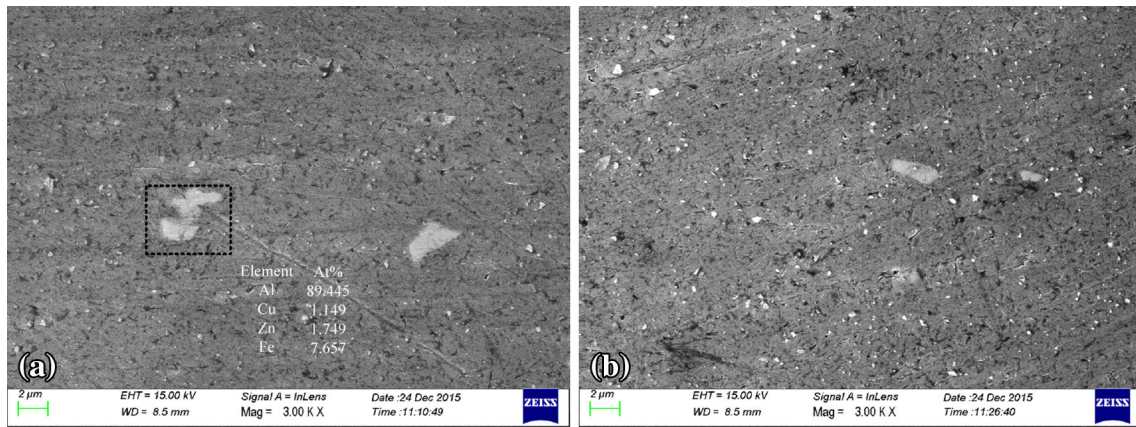
Fig. 7 Constituent particles of BM and NZ of joint at the welding speed of 30 mm/min: (a) BM and (b) NZ

BM in Fig. 7(a), the coarse precipitation particles are easily broken into smaller particles by rotational tool and then redistributed randomly (Fig. 7b).

3.3 Mechanical Properties of Joint

Hardness distribution of SSFSW joint at the welding speed of 30 mm/min was investigated and the results of two specimens are shown in Fig. 8. It is seen that hardness distribution of joint presents typical W-shape, while the lowest hardness value of 100Hv locates in HAZ of AS and the highest value lies in BM. As a matter of fact, 7N01-T4 alloy is a precipitate strengthening alloy, whose hardness is not only related to distribution and size of strengthening particles, but also affected by grain size (Ref 1, 19-22). Compared to BM, the HAZ consisting of coarser grains owns lower hardness value. The material in TMAZ is acted by stirring action, which results in smaller grain size and higher dislocation density than HAZ (Ref 23). Therefore, compared with HAZ, TMAZ owns higher hardness value. It is known that the smaller the grain size, the higher the hardness (Ref 4, 19). Therefore, the hardness of NZ characterized by fine and equiaxed grains is higher than that of TMAZ.

In this study, tensile tests were performed and engineering stress and strain diagram of joint under different rotational tool is shown in Fig. 9. Mechanical properties of tensile specimens of BM and joint obtained under different welding speeds are shown in Fig. 10. As a matter of fact, the frictional heat is mainly generated by inner rotational tool during the welding process, while the outer stationary shoulder can quickly cool the joint and then may lead to insufficient flow behavior, which has been reported by Li et al. (Ref 4). In addition, it is worth mentioning that the flow ability of 7000 series aluminum alloys is worse than 6000 series alloys. Therefore, higher heat input is indispensable to higher strength of joint. However, too high frictional heat is not beneficial to the increase of mechanical properties, which is attributed to the softening of joint. In this study, the defect-free joint with high mechanical properties is produced at 20 mm/min. As the welding speed increase to 30 mm/min, the heat input decreases, which is propitious to reduce the softening of joint and then attain higher mechanical properties. With the increase of welding speed to 40 and 50 mm/min, the mechanical property of joint decreases, which is attributed to defect near the interface between NZ and TMAZ. When the welding speed reaches 70 mm/min, the
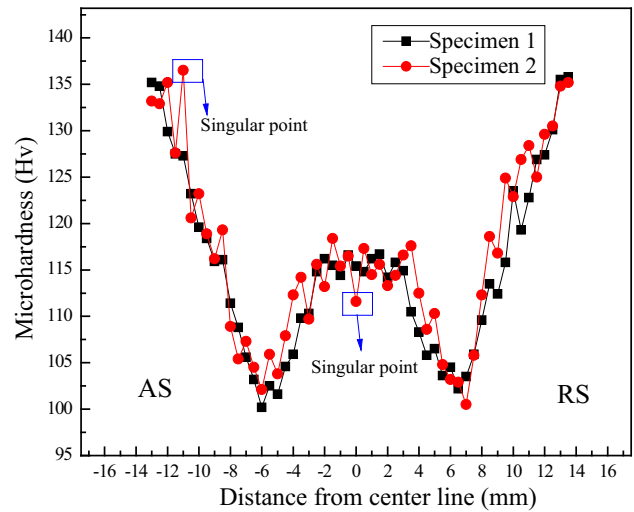

Fig. 8 Microhardness distribution of joint under the welding speed of 30 mm/min and rotational velocity of 2000 rpm
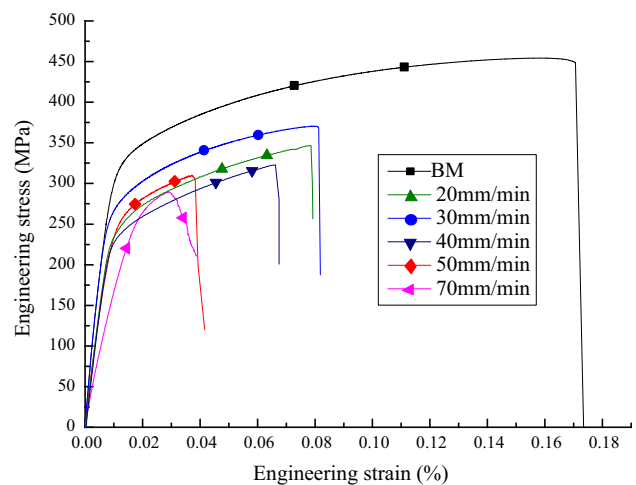

Fig. 9 Engineering stress and strain of BM and joints under different welding speeds

cavity defect forms in the joint, leading to the drastic reduction of mechanical property. Therefore, it can be concluded that tensile strength and elongation of SSFSW joint firstly increase and then decease with the increase of welding speed, which are all lower than BM. At the welding speed of 30 mm/min and rotational velocity of 2000 rpm, the tensile strength and elongation of joint reach 379 MPa and 7.9%, equivalent to 84.2 and 52% of BM, respectively. The tensile strength is much higher than those reported by Meng et al. and Han et al. (Ref 6, 7). Therefore, it can be expounded that stationary shoulder is more suitable to weld 7N01-T4 aluminum alloy, which can not only obtain smooth surface but also improve mechanical properties.

Figure 11 exhibits the fracture positions of SSFSW joints using different welding speeds. In fact, the tensile fracture of FSW joint is closely related to defect position or minimum hardness location (Ref 19). Tensile fracture of defect-free joint at 20 or 30 mm/min mainly depends on minimum hardness location. During SSFSW process, the HAZ of joint experiences over aging, which results in softening phenomenon of joint. In this study, the fracture locations of joints at 20 mm/min and 30 mm/min both locate at HAZ of AS (Fig. 11), which agrees
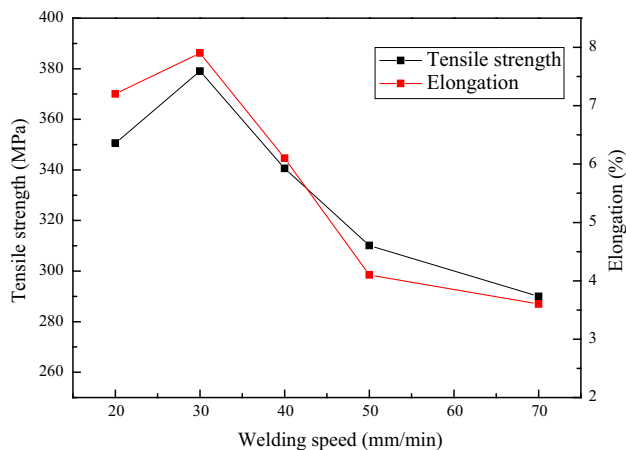
with the hardness distribution of joint (Fig. 8). With the further increase of welding speed, fracture location is mainly related to the defect appearing in the welding joint, as shown in Fig. 11(c)-(e). The defect can lead to stress concentration and decrease of load bearing, deteriorating mechanical properties of joint (Ref 24).

Figure 12 exhibits the fracture surface morphologies of BM and joints using different welding speeds. It is seen that the fracture surfaces of tensile specimens are characterized by various size dimples, presenting typical ductile fracture. As indicated in Fig. 12(a), there are some larger and deeper dimples on the fractures surface of BM. During SSFSW process, the heat input has a significant effect on SSFSW joint, which leads to the variations of facture surface morphology. For the joint at 20 mm/min, the fracture surface is covered with smaller and shallower dimples (Fig. 12b). At 30 mm/min, there are some large and deep dimples in fracture surface of joint, while some cracked second-phase particle at the bottom, which shows good ductility and tensile strength, as indicated in Fig. 12(c). As the welding speed further increases to 40, 50, or 70 mm/min, tensile fracture of joint is mainly influenced by the defect. Therefore, fracture surface morphologies of these joints are not given.

4. Conclusions

The SSFSW of 7N01-T4 aluminum alloy was carried out and effects of welding speed on surface formation, microstructures, and mechanical properties of joint were investigated. On the basis of present investigation, the following conclusions can be extracted:

(1) For 7N01-T4 aluminum alloy owning lower heat conductivity, decreasing welding speed is beneficial to soften SSAZ and then obtain smooth surface of joint.

(2) Under the constant rotational velocity of 2000 rpm, defect-free SSFSW joints are obtained using the welding speeds of 20 mm/min and 30 mm/min. Increasing welding speed may result in the appearance of defect near the interface between RSAZ and TMAZ. In addition, compared with clockwise rotation, anti-clockwise rota-
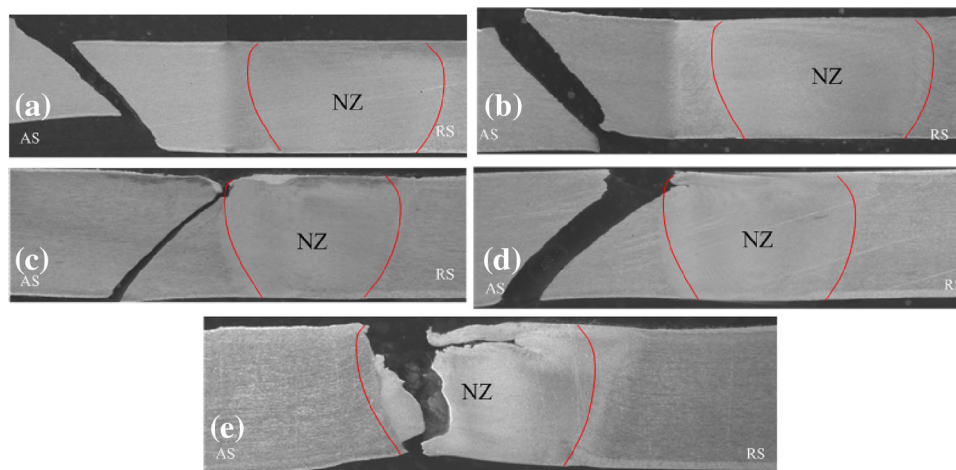

Fig. 10 Tensile strength and elongation of joints under different welding speeds

Fig. 11 Fracture locations of joints using different welding speeds: (a) 20 mm/min, (b) 30 mm/min, (c) 40 mm/min, (d) 50 mm/min, and (e) 70 mm/min
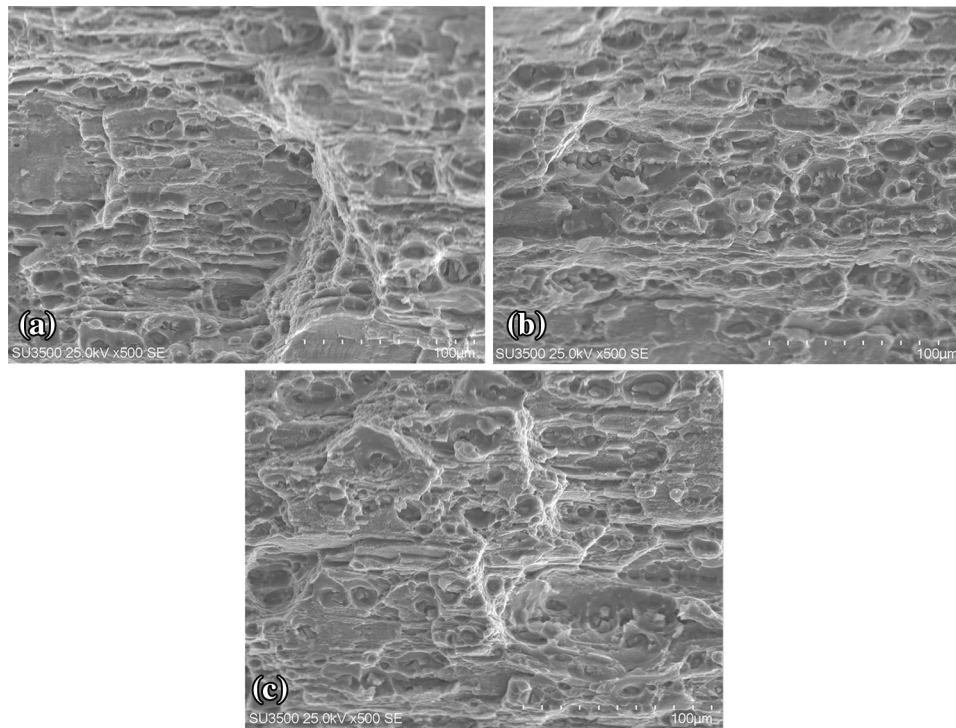
Fig. 12 Fracture surfaces of tensile specimens: (a) BM, (b) 20 mm/min, and (c) 30 mm/min

tion of tool is more propitious to improve formation of joint for tool pin with right screw.

(3) With the increase of welding speed, the tensile strength and elongation of joint increase first and then decrease. When the welding speed is 30 mm/min, the tensile strength and elongation of joint reach maximum values of 379 MPa and 7.9%, up to 84.2 and 52% of BM, respectively. Moreover, fracture surface consists of many dimples with various sizes, indicating typical ductile fracture.

Reference

1. R.S. Mishra and Z.Y. Ma, Friction Stir Welding and Processing, *Mater. Sci. Eng. R.*, 2005, **50**, p 1–78
2. N. Oiwa, S. Iwaki, T. Okada, N. Eguchi, S. Tanaka, and K. Namba, Studies on Characteristics of Friction Stir Welded Joints in Structural Thin Aluminium Alloys Part 1: Imperfections in Friction Stir Welded Zones and Their Precision Non-destructive Testing, *Weld. World*, 2005, **49**(3–4), p 76–82
3. T. Okada, H. Hori, T. Hashimoto, H. Tanikawa, S. Iwaki, J. Takeda, T. Miyamichi, N. Eguchi, S. Tanaka, N. Oiwa, and K. Namba, Studies on Characteristics of Friction Stir Welded Joints in Structural Thin Aluminium Alloys Part 2: Metallurgical Features and Mechanical Properties of Friction Stir Welded Joints, *Weld. World*, 2005, **49**(3–4), p 83–92
4. D.X. Li, X.Q. Yang, L. Cui, F.Z. He, and X. Zhang, Investigation of Stationary Shoulder Friction Stir Welding of Aluminum alloy 7075-T651, *J. Mater. Process. Technol.*, 2015, **222**, p 391–398
5. H.J. Zhang, H.J. Liu, and L. Yu, Effect of Water Cooling on the Performances of Friction Stir Welding Heat-Affected Zone, *J. Mater. Eng. Perform.*, 2012, **21**(7), p 1182–1187
6. L.C. Meng, X. Kang, Y.J. Sun, K. Sun, and Q.Y. Shi, Mechanical Properties of 7N01 Aluminum Alloy Friction Stir Welding Joint, *Trans. China Weld Ins.*, 2012, **33**(2), p 90–92 **(in Chinese)**
7. K.V. Jata, K.K. Sankaran, and J.J. Ruschau, Friction-Stir Welding Effects on Microstructure and Fatigue of Aluminum Alloy 7050-T7451, *Metall. Mater. Trans. A.*, 2012, **31**(9), p 2181–2192
8. J.Q. Li and H.J. Liu, Effects of Tool Rotation Speed on Microstructures and Mechanical Properties of AA2219-T6 Welded by the External Non-rotational Shoulder Assisted Friction Stir Welding, *Mater. Des.*, 2013, **43**, p 299–306
9. J.Q. Li and H.J. Liu, Design of Tool System for the External Nonrotational Shoulder Assisted Friction Stir Welding and Its Experimental Validations on 2219-T6 Aluminum Alloy, *Int. J. Adv. Manuf. Technol.*, 2013, **66**, p 623–634
10. D.X. Li, X.Q. Yang, L. Cui, F.Z. He, and H. Shen, Effect of Welding Parameters on Microstructure and Mechanical Properties of AA6061-T6 Butt Welded Joints by Stationary Shoulder Friction Stir Welding, *Mater. Des.*, 2014, **64**, p 251–260
11. S.D. Ji, X.C. Meng, L. Ma, H. Lu, and S.S. Gao, Vertical Compensation Friction Stir Welding Assisted by External Stationary Shoulder, *Mater. Des.*, 2015, **68**, p 72–79
12. GB/T 6394-2002. Metal-methods for estimating the average grain size
13. GB/T 2651-2008. Destructive tests on welds in metallic materials-transverse tensile test
14. Y.J. Chao, X. Qi, and W. Tang, Heat Transfer in Friction Stir Welding—Experimental and Numerical Studies, *J. Manuf. Sci. Eng.*, 2003, **125**(1), p 138–145
15. R. Nandan, G.G. Roy, and T. Debroy, Numerical Simulation of Three-Dimensional Heat Transfer and Plastic Flow During Friction Stir Welding, *Metall. Mater. Trans. A.*, 2006, **37A**, p 1247–1259
16. L.M. Ke, J.L. Pan, L. Xing, and S.L. Wang, Sucking-Extruding Theory for the Material Flow in Friction Stir Welds, *J. Mech. Eng.*, 2009, **45**(4), p 89–94 **(in Chinese)**

17. L. Wan, Y. Huang, Z. Lv, S. Lv, and J. Feng, Effect of Self-Support Friction Stir Welding on Microstructure and Microhardness of 6082-T6 Aluminum Alloy Joint, *Mater. Des.*, 2014, **55**, p 197–203

18. S.D. Ji, X.C. Meng, J.G. Liu, L.G. Zhang, and S.S. Gao, Formation and Mechanical Properties of Stationary Shoulder Friction Stir Welded 6005A-T6 Aluminum Alloy, *Mater. Des.*, 2014, **62**, p 113–117

19. Y.X. Huang, L. Wan, S.X. Lv, and J.C. Feng, Novel Design of Tool for Joining Hollow Extrusion by Friction Stir Welding, *Sci. Technol. Weld. Joining.*, 2013, **18**(3), p 239–246

20. P. Dong, H.M. Li, D.Q. Sun, W.B. Gong, and J. Liu, Effects of Welding Speed on the Microstructure and Hardness in Friction Stir Welding Joints of 6005A-T6 Aluminum Alloy, *Mater. Des.*, 2013, **45**, p 524–531

21. J.Q. Su, T.W. Nelson, R. Mishra, and M. Mahoney, Microstructural Investigation of Friction Stir Welded 7050-T651 Aluminium, *Acta Mater.*, 2003, **51**(3), p 712–729

22. J.Q. Su, T.W. Nelsona, and C.J. Sterling, Microstructure Evolution During FSW/FSP of High Strength Aluminum Alloys, *Mater. Sci. Eng. A.*, 2005, **405**(1–2), p 277–286

23. H.J. Aval, S. Serajzadeh, N.A. Sakharova, A.H. Kokabi, and A. Loureiro, A Study on Microstructures and Residual Stress Distributions in Dissimilar Friction-Stir Welding of AA5086–AA6061, *J. Mater. Sci.*, 2012, **47**(12), p 5428–5437

24. D.R. Ni, D.L. Chen, B.L. Xiao, D. Wanga, and Z.Y. Ma, Residual Stresses and High Cycle Fatigue Properties of Friction Stir Welded SiCp/AA2009 Composites, *Int. J. Fatigue.*, 2013, **55**, p 64–73